

Correlations generated from high-temperature states: Nonequilibrium dynamics in the Fermi-Hubbard model

Ian G. White,^{*} Randall G. Hulet, and Kaden R. A. Hazzard
Department of Physics and Astronomy, Rice University, Houston, Texas 77005, USA
and Rice Center for Quantum Materials, Rice University, Houston, Texas 77005, USA

 (Received 28 May 2019; published 16 September 2019)

We study interaction quenches of the Fermi-Hubbard model initiated from various high-temperature and high-energy states, motivated by cold atom experiments, which currently operate above the ordering temperature(s). We analytically calculate the dynamics for quenches from these initial states, which are often strongly interacting, to the noninteracting limit. Even for high-temperature uncorrelated initial states, transient connected correlations develop. These correlations share many features for all considered initial states. We observe light-cone spreading of intertwined spin and density correlations. The character of these correlations is quite different from their low-temperature equilibrium counterparts: for example, the spin correlations can be ferromagnetic. We also show that an initially localized hole defect affects spin correlations near the hole, suppressing their magnitude and changing their sign.

DOI: [10.1103/PhysRevA.100.033612](https://doi.org/10.1103/PhysRevA.100.033612)

I. INTRODUCTION

The development of correlations out of equilibrium is the topic of much recent research in atomic, molecular, and optical (AMO) and condensed-matter systems. Major areas of interest include the relaxation dynamics of a system driven out of equilibrium [1–15] and the possibility of relaxation to nonthermal steady states [16–29] that have unusual properties [19,30–39]. An emerging direction involves inducing nonequilibrium correlations at temperatures above those required for equilibrium order. This is especially relevant given the recently demonstrated ability to probe and control nonequilibrium dynamics in solid-state systems using optical pulses [40–43]. However, numerous questions exist regarding the dynamics after quenches: What conditions are required for correlations to develop? What timescales are involved? What will the character of these correlations be?

In this paper we study quenches of the Fermi-Hubbard model from finite (and in some cases very high) initial temperatures to noninteracting final Hamiltonians. This is a useful complement to studies that consider dynamics from low-temperature initial conditions [5,7,28,44,45]. Besides its intrinsic interest, this regime is important to ongoing experiments. This is because, despite much recent progress towards realizing low-temperature equilibrium states experimentally, the regime well below the ordering temperatures (e.g., the Néel temperature for the antiferromagnet) remains elusive due to the very low temperatures and entropies required [46–65]. Furthermore, sudden quench dynamics of interaction and tunneling parameters provide a useful comparison to the finite-time quench dynamics which are being investigated

with the aim of cooling lattice fermions and preparing an antiferromagnetic ground state [66–68].

We find that, even when initiated from high-temperature initial states that are above the superexchange or even tunneling energy scales, such quenches generate transient particle number and spin correlations between two sites; after the quench a light cone of connected correlations between increasingly distant sites develops over time. A wide range of initial product states exhibit qualitatively similar correlation dynamics. In particular we calculate the dynamics for high-temperature Mott insulators in one and two dimensions, a strongly interacting metal, a partially spin-polarized Mott insulator, and a perfect product state antiferromagnet.

The transient correlations can be qualitatively different from the correlations of the equilibrium low-temperature states of the same initial Hamiltonian. For example, we observe the generation of ferromagnetic spin correlations from a Hamiltonian with initially repulsive on-site interactions, in contrast to the antiferromagnetic spin correlations that occur in equilibrium for the repulsive Hubbard model.

Going forward, our results will help one understand quenches with finite interactions after the quench. On the one hand, when phenomena persist with interactions, our results provide a foundation for understanding them. On the other hand, when interactions lead to phenomena that are absent in our results, it signals that the physics is intrinsically interacting. Given how surprising out-of-equilibrium dynamics can be, it is crucial to sort out which surprises result from the interactions and which arise from the inherent nonequilibrium nature of the problem.

An example drives this home. Imagine that one found that spin and density correlations were evolving dynamically with exactly the same magnitude. This intriguing behavior is reminiscent of “intertwined” spin and density order in equilibrium strongly correlated systems [69]. Although a natural instinct

^{*}igw2@rice.edu

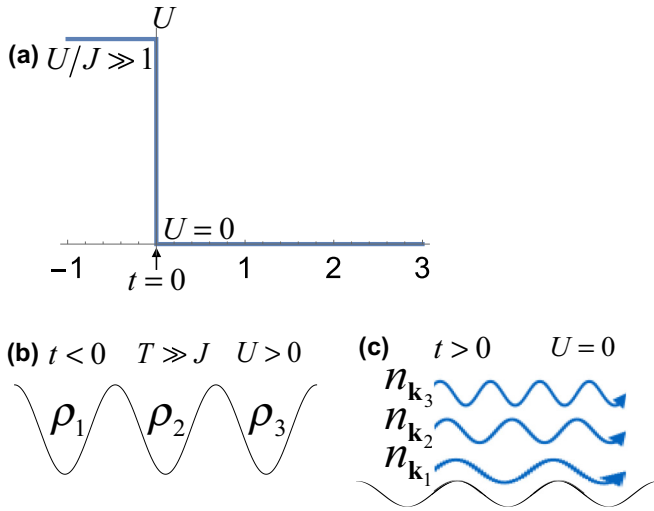


FIG. 1. (a) Quench protocol for the dynamics in this paper (arbitrary units). (b) Prequench, the system is in a product of single-site states. An important class of states of this form that we consider arise from the $J_0 \ll T \ll U_0$ equilibrium state of the Fermi-Hubbard Hamiltonian. (c) Postquench, the system evolves in the noninteracting limit of the Fermi-Hubbard Hamiltonian, with conserved momentum occupation numbers.

is to imagine that this observation is similarly nontrivial, one of our results is to show that such dynamics occurs even for noninteracting quenches. Comparing to this important baseline allows one to assess how significant a given observation in a strongly interacting system really is.

We also study the transport of a hole defect after a quench. We show that, as the hole propagates, it affects the development of correlations around it. Superficially, it appears that the hole is dressed with a cloud of spin correlations. This is another example where, if this were observed in a strongly interacting system, one might draw the conclusion that the physics was highly nontrivial, but in fact the richness here appears already in the noninteracting dynamics.

This paper is organized as follows: Section II describes how we calculate the dynamics of observables quenched from initial spatial product states to noninteracting Hamiltonians. Section III applies the theory to calculate the connected correlations in a one-dimensional Mott insulator. Section IV shows that qualitatively similar phenomena persist for multiple initial conditions. Section V describes how an initially localized hole defect modifies the dynamics of spin correlations. Section VI presents conclusions and outlook.

II. QUENCH DYNAMICS IN THE NONINTERACTING LIMIT

We consider interaction quenches from initial product states to the noninteracting limit for ultracold fermions in an optical lattice, illustrated in Fig. 1. The initial state is

$$\rho = \bigotimes_i \rho_i^{(1)}, \quad (1)$$

where $\rho_i^{(1)}$ is an arbitrary density matrix for site i (in general a mixed state).

In a deep lattice, this system is described by the Hubbard Hamiltonian

$$H = -J \sum_{\langle ij \rangle, \alpha} c_{i\alpha}^\dagger c_{j\alpha} + U \sum_i n_{i\uparrow} n_{i\downarrow}, \quad (2)$$

where $\langle ij \rangle$ indicates a nearest-neighbor pair of sites, $\alpha \in \{\uparrow, \downarrow\}$, $c_{i\alpha}$ is the fermionic annihilation operator at site i with spin α , and $n_{i\alpha} = c_{i\alpha}^\dagger c_{i\alpha}$ is the corresponding number operator. Equation (2) models fermions with a nearest-neighbor tunneling amplitude $J > 0$ and on-site interaction energy U [70–72]. Many of our initial states arise as high-temperature ($T \gg J_0$) equilibrium states of Eq. (2), and the postquench dynamics is governed by its $U = 0$ limit. This single-band model suffices to capture many equilibrium scenarios in ultracold matter, and we discuss below its applicability to the nonequilibrium quenches that we consider in this work.

Figure 1 illustrates our quench protocol, in which the system starts in equilibrium at some value of U and the interaction is turned off at $t = 0$:

$$U(t) = U_{\text{init}}[1 - \Theta(t)], \quad (3)$$

where Θ is the Heaviside step function and $|U_0| \gg J_0$. When the temperature T before the quench is large compared with J_0 (the tunneling before the quench)—i.e., $T \gg J_0$ —the initial state takes the form of Eq. (1) (we consider a few alternative product states later). Experimentally, the interaction can be dynamically controlled by using a Feshbach resonance or changing the lattice depth. Each method has strengths and limitations for realizing interaction quenches that we will discuss at the end of this section.

We note that our calculations actually describe a variety of more general quenches of the Fermi-Hubbard model. The only required conditions are that the initial temperature T satisfies $T \gg J_0$ and $U = 0$ after the quench. So, for example, one could suddenly change both U and J at time $t = 0$ as long as these conditions are met.

Our goal is to calculate the density and spin expectation values and two-site correlation functions for $t > 0$. We define on each site the total density operator $n_i = \sum_\alpha n_{i\alpha}$ and the spin operators $\vec{\sigma}_i = \sum_{\alpha\beta} c_{i\alpha}^\dagger \vec{\sigma}_{\alpha\beta} c_{i\beta}$, where $\vec{\sigma}_{\alpha\beta}$ is the vector of Pauli matrices. We focus on these observables as the most basic correlations that characterize equilibrium systems, and because some or all of them can be measured in experiments by a variety of methods; for example, direct observation with quantum gas microscopes [57,58,73,74] and detection by Bragg scattering [47], modulation spectroscopy [75], reconstruction from *in situ* imaging [64], manipulation of a superlattice [76], or detection of noise correlations [77,78].

Note that the correlation functions can be expressed as

$$\langle n_i n_j \rangle = \sum_{\alpha\beta} \langle c_{i\alpha}^\dagger c_{i\alpha} c_{j\beta}^\dagger c_{j\beta} \rangle, \quad (4)$$

$$\langle \sigma_i^a \sigma_j^b \rangle = \sum_{\alpha\beta\gamma\delta} \sigma_{\alpha\beta}^a \sigma_{\gamma\delta}^b \langle c_{i\alpha}^\dagger c_{i\beta} c_{j\gamma}^\dagger c_{j\delta} \rangle, \quad (5)$$

where $a, b \in \{x, y, z\}$. Therefore, we turn to calculating the dynamics of a general two-site correlation $\langle c_{i\alpha}^\dagger c_{i\beta} c_{j\gamma}^\dagger c_{j\delta} \rangle$, from which we can obtain the density and spin correlations. For compactness, we define

$$C_{ij}^{nm} = \langle n_i n_j \rangle - \langle n_i \rangle \langle n_j \rangle, \quad (6)$$

$$C_{ij}^{ab} = \langle \sigma_i^a \sigma_j^b \rangle - \langle \sigma_i^a \rangle \langle \sigma_j^b \rangle, \quad (7)$$

where $a, b \in \{x, y, z\}$.

Because the Hamiltonian after the quench is noninteracting, one can analytically express the time-evolution of the annihilation operator at site j as

$$c_{j\alpha}(t) = \sum_l A_{jl}(t) c_{l\alpha}, \quad (8)$$

where $A_{jl}(t)$ is the propagator from site l to site j of a single particle on the lattice. Equation (8) follows because our Hamiltonian can be written $H = \sum_{k\alpha} \mathcal{E}_k b_{k\alpha}^\dagger b_{k\alpha}$ for some set of annihilation operators $b_{k\alpha}$, which annihilate atoms with spin α in single-particle eigenstates indexed by k . (For translationally invariant systems, k is the quasimomentum.) The time evolution of these operators is $b_{k\alpha}(t) = e^{-i\mathcal{E}_k t} b_{k\alpha}$. If no time argument is provided, the operator is evaluated at $t = 0$, and we set $\hbar = 1$ throughout. The position-space annihilation operators $c_{j\alpha}$ can be expressed as $c_{j\alpha} = \sum_k S_{jk} b_{k\alpha}$ for some S_{jk} . Conversely, $b_{k\alpha} = \sum_j (S^{-1})_{kj} c_{j\alpha}$. Hence, at time t , $c_{j\alpha}(t) = \sum_k S_{jk} b_{k\alpha}(t) = \sum_k S_{jk} e^{-i\mathcal{E}_k t} b_{k\alpha} = \sum_{kl} e^{-i\mathcal{E}_k t} S_{jk} (S^{-1})_{kl} c_{l\alpha}$.

In one dimension the single-particle eigenstates k can be identified with quasimomentum states in the first Brillouin zone, for which $\mathcal{E}_k = -2J \cos(ka)$ and $S_{jk} = \exp(ijka)/\sqrt{N}$.

Taking $N \rightarrow \infty$ we see that Eq. (8) holds with

$$A_{jl}(t) = (-i)^{|j-l|} \mathcal{J}_{|j-l|}(2Jt), \quad (9)$$

where $\mathcal{J}_m(z)$ is a Bessel function of the first kind.

The expectation value of the general single-site density-matrix element at time t is given in terms of initial expectation values by

$$\langle c_{i\alpha}^\dagger(t) c_{i\beta}(t) \rangle = \sum_{p,q} A_{ip}^*(t) A_{iq}(t) \langle c_{p\alpha}^\dagger c_{q\beta} \rangle_0, \quad (10)$$

while the general two-site correlator that determines the density and spin correlations at time t is given by

$$\begin{aligned} \langle c_{i\alpha}^\dagger(t) c_{i\beta}(t) c_{j\gamma}^\dagger(t) c_{j\delta}(t) \rangle \\ = \sum_{p,q,r,s} A_{ip}^*(t) A_{iq}(t) A_{jr}^*(t) A_{js}(t) \langle c_{p\alpha}^\dagger c_{q\beta} c_{r\gamma}^\dagger c_{s\delta} \rangle_0, \end{aligned} \quad (11)$$

using Eq. (8), where $\langle \dots \rangle_0$ indicates the expectation value at time $t = 0$.

We compute these initial expectation values by taking advantage of the product-state nature of Eq. (1). In this state, expectation values of operators factor by site: $\langle P_i Q_j \rangle_0 = \langle P_i \rangle_0 \langle Q_j \rangle_0$ if $i \neq j$ for operators P_i and Q_j supported on single sites. Then Eq. (10) simplifies to

$$\langle c_{i\alpha}^\dagger c_{i\beta} \rangle(t) = \sum_p |A_{ip}(t)|^2 \langle c_{p\alpha}^\dagger c_{p\beta} \rangle_0. \quad (12)$$

Likewise, Eq. (11) factors into a sum of three types of non-vanishing terms: (i) $p = q = r = s$, (ii) $p = q$ and $r = s$ with $p \neq r$, and (iii) $p = s$ and $r = q$ with $p \neq r$. Writing the expectation in terms of these sums (and renaming summation indices), we have

$$\begin{aligned} \langle c_{i\alpha}^\dagger c_{i\beta} c_{j\gamma}^\dagger c_{j\delta} \rangle(t) = \sum_p |A_{ip}(t)|^2 |A_{jp}(t)|^2 \langle c_{p\alpha}^\dagger c_{p\beta} c_{p\gamma}^\dagger c_{p\delta} \rangle_0 + \sum_{p \neq q} |A_{ip}(t)|^2 \langle c_{p\alpha}^\dagger c_{p\beta} \rangle_0 |A_{jq}(t)|^2 \langle c_{q\gamma}^\dagger c_{q\delta} \rangle_0 \\ + \sum_{p \neq q} A_{ip}^*(t) A_{jp}(t) \langle c_{p\alpha}^\dagger c_{p\beta} \rangle_0 A_{iq}(t) A_{jq}^*(t) \langle c_{q\beta}^\dagger c_{q\gamma} \rangle_0. \end{aligned} \quad (13)$$

Although the last two terms are double sums over p and q with $p \neq q$, the summand factors. The sums can be written as products of single sums because in general $\sum_{p \neq q} P_p Q_q = \sum_{p,q} P_p Q_q - \sum_p P_p Q_p$. Using this, and using $\langle c_{p\alpha}^\dagger c_{p\beta} \rangle_0 = \delta_{\alpha\beta} - \langle c_{p\beta}^\dagger c_{p\alpha} \rangle_0$ to write each expectation value in a structurally similar form allows us to rewrite Eq. (13) as

$$\begin{aligned} \langle c_{i\alpha}^\dagger c_{i\beta} c_{j\gamma}^\dagger c_{j\delta} \rangle(t) = \sum_p |A_{ip}(t)|^2 |A_{jp}(t)|^2 [g_{\alpha\beta\gamma\delta}^p - f_{\alpha\beta}^p f_{\gamma\delta}^p - f_{\alpha\delta}^p (\delta_{\beta\gamma} - f_{\gamma\beta}^p)] + \left[\sum_p |A_{ip}(t)|^2 f_{\alpha\beta}^p \right] \left[\sum_q |A_{jq}(t)|^2 f_{\gamma\delta}^q \right] \\ + \left[\sum_p A_{ip}^*(t) A_{jp}(t) f_{\alpha\delta}^p \right] \left[\sum_q A_{iq}(t) A_{jq}^*(t) (\delta_{\beta\gamma} - f_{\gamma\beta}^q) \right]. \end{aligned} \quad (14)$$

We have defined

$$f_{\alpha\beta}^i = \langle c_{i\alpha}^\dagger c_{i\beta} \rangle_0, \quad (15a)$$

$$g_{\alpha\beta\gamma\delta}^i = \langle c_{i\alpha}^\dagger c_{i\beta} c_{i\gamma}^\dagger c_{i\delta} \rangle_0, \quad (15b)$$

to simplify notation. These are the general one-particle and two-particle correlation functions on a single site.

With this rearrangement, double sums are eliminated (they factor) and only single sums remain. In combination with

Eqs. (4) and (5), this allows the time evolution of the density-density and spin-spin correlators to be calculated efficiently. With Eqs. (12) and (14) C_{ij} can then be calculated. It should be emphasized that the steps leading to Eqs. (12) and (13) are only valid for initial states that are products over single sites.

We note that our calculations are similar to those by Gluza *et al.* in Ref. [79] who also study noninteracting lattice fermions. Their focus is on the generic properties of

thermalization, independent of the initial state or details of the noninteracting postquench Hamiltonian. We consider a concrete, physically relevant Hamiltonian and initial states and focus on interesting phenomena that occur during the transient dynamics.

We now consider the experimental feasibility and challenges of quenching U to zero on a timescale much faster than J^{-1} . Two possible methods are to change the scattering length using a Feshbach resonance or to change U/J by changing the lattice depth.

Controlling the scattering length with a Feshbach resonance allows U to be tuned over a wide range, independently of J . Although ramping across a magnetic Feshbach resonance from the strongly interacting regime to approximately zero scattering length within this timescale is an experimental challenge due to the finite response time of the magnetic-field coils, Ref. [80] demonstrates that such a quench is possible, with a ramp time on the order of $5 \mu\text{s}$. In experiments that cannot quench so rapidly, we expect the qualitative phenomena that we have predicted to persist to ramp times $t \sim J^{-1}$. In fact, one can think of the postquench evolution as proceeding from a modified initial state; a scenario that we discuss at the end of the next section.

In contrast, quenching U/J by decreasing the optical lattice depth can be done much faster than J^{-1} , and a broad range of U/J can be achieved. An example of the range of attainable values of U/J can be seen in Ref. [81]. However, with this method it is difficult to achieve $U_{\text{final}} \ll J$ while maintaining a single-band nearest-neighbor Hamiltonian. For typical values of scattering length and lattice spacing, for example, as in Ref. [81], one can reach postquench $U/J \sim 0.5$ while remaining reasonably in the tight-binding limit. Werner *et al.* in Ref. [82] compute the region of validity of the single-band Hubbard model for lattice fermions and also find that one can achieve $U/J < 1$ but not strictly $U/J = 0$.

For somewhat short times $t \ll U^{-1}$, we expect our predictions to be accurate, and for the qualitative predictions to hold out to $t \sim U^{-1}$. However, the steady state can be drastically altered, with the interactions breaking integrability and causing long-time thermalization to an equilibrium state of the interacting Hamiltonian. For small final U/J the energy imparted to the system by the quench is extremely large, so the final steady state should be a very-high-temperature state without significant correlations.

III. QUENCH FROM $T \gg J$ MOTT INSULATOR

We now apply the results of Sec. II to a Mott insulating initial state. Before proceeding, we first discuss the applicability of the description developed in Sec. II to current experiments.

Most of the initial states we consider in this work are product states satisfying $J_0 \ll T \ll U_0$, so we consider the feasibility of reaching $J_0 \ll T$, especially while simultaneously satisfying $T \ll U_0$, and examine the corrections to the dynamics if this does not hold. Temperatures $T \ll U$ have been realized in multiple experiments discussed in Sec. I. The remaining criterion is to reach such low T/U in a regime where $J \ll T$. Although equilibration with such low J can be challenging, the expected energy scales should allow this, and in fact recent experiments have reached this regime.

For example, in Ref. [81] Cheuk *et al.* characterize a Mott insulator with $U/8J \approx 12$, $T/U \approx 0.09$, and $S/N \approx 1.23k_B$.

Experiments will always deviate from a perfect $J = 0$ product state, so we qualitatively consider the effect of an initial tunneling amplitude J_0 much less than U_0 or T . For small but nonzero J_0 , expectation values in the initial equilibrium state will in general have $O(J_0/T)$ corrections. Many expectation values, such as the two-site density-density and spin-spin correlations, have smaller $O((J_0/T)^2)$ corrections since the tunneling matrix element vanishes between the $J = 0$ eigenstates. The postquench dynamics are still exactly solvable, and the sole effect of the imperfect initial product state is to require one to use Eqs. (10) and (11) directly. Although it is not possible to evaluate the expectation values in these equations in general, it is clear that the $O(J_0/T)$ corrections in the initial state directly translate to $O(J_0/T)$ corrections in the dynamics (and likewise for higher orders). Because the dynamics is integrable, we expect that the steady state will in general be nonthermal and will likely be described by a generalized Gibbs ensemble (GGE).

We now consider a Mott insulating initial state with $U_0 \gg T \gg J_0$, no spin polarization, and unit filling enforced by choosing the chemical potential to be $\mu = U_0/2$. We write $H = \sum_i H_i$ with

$$H_i = U_0 n_{i\uparrow} n_{i\downarrow} - \mu n_i. \quad (16)$$

In this limit, the density matrix is given by

$$\begin{aligned} \rho &= Z^{-1} \exp(-\beta H) \\ &= Z^{-1} \exp\left(-\beta \sum_i H_i + O(J_0/T)\right) \\ &\approx Z^{-1} \bigotimes_i \exp(-\beta H_i), \end{aligned} \quad (17)$$

where Z is a constant enforcing $\text{Tr} \rho = 1$, $\beta = 1/T$ is the inverse temperature, and we set $k_B = 1$ throughout.

In what follows, we associate with any energy A a dimensionless ratio $\tilde{A} = \beta A$. Then the expectation values f and g from Eq. (15) in the initial state are

$$f_{\alpha\beta}^i = \frac{1}{2} \delta_{\alpha\beta}, \quad (18a)$$

$$g_{\alpha\beta\gamma\delta}^i = \begin{cases} \frac{1}{2} & \alpha = \beta = \gamma = \delta \\ \frac{1}{2} \frac{1}{1+e^{\frac{1}{2}\tilde{U}_0}} & \alpha = \beta \neq \gamma = \delta \\ \frac{1}{2} \left(1 - \frac{1}{1+e^{\frac{1}{2}\tilde{U}_0}}\right) & \alpha = \delta \neq \beta = \gamma \\ 0 & \text{otherwise,} \end{cases} \quad (18b)$$

Figure 2 shows the postquench correlation dynamics of this $T \gg J_0$ Mott insulating initial state obtained by Eqs. (4), (5), and (14) using $f_{\alpha\beta}^i$ and $g_{\alpha\beta\gamma\delta}^i$ given in Eq. (18), with $T \ll U_0$. The results are independent of U_0 and J_0 so long as this inequality is satisfied. For a fixed distance, transient connected correlations develop after the quench. Connected correlations of both spin [Figs. 2(a) and 2(c)] and density [Figs. 2(b) and 2(d)] develop as a function of time in the shape of a light cone: correlations develop inside, and at the edge of, a region in space whose size grows as vt for some velocity v . We observe that connected correlations spread at a

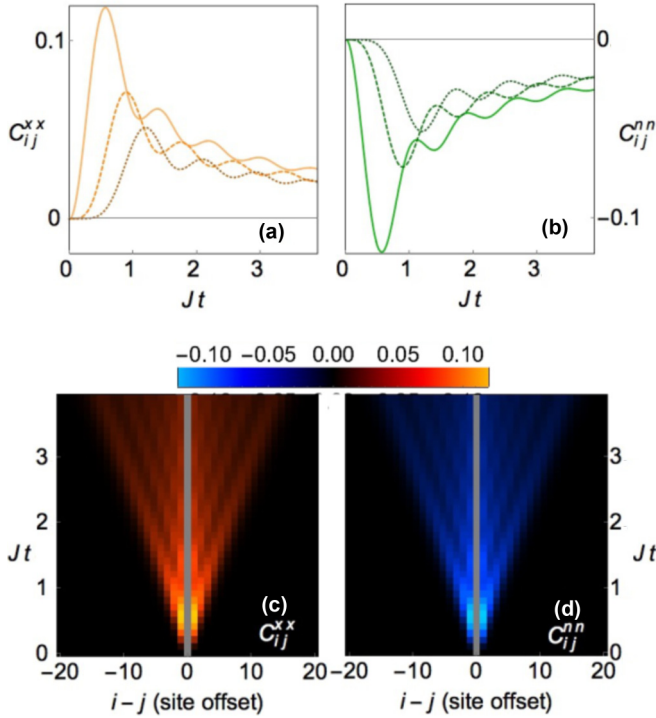


FIG. 2. Connected correlations of a $J_0 \ll T \ll U_0$ 1D Mott insulator quenched to a noninteracting Hamiltonian. (a) Spin-spin correlations $C_{ij}^{xx} = \langle \sigma_i^x \sigma_j^x \rangle - \langle \sigma_i^x \rangle \langle \sigma_j^x \rangle$ and (b) density-density correlations $C_{ij}^{nn} = \langle n_i n_j \rangle - \langle n_i \rangle \langle n_j \rangle$ between sites with an offset of one (solid lines), two (dashed lines), or three (dotted lines). (c) Spin-spin and (d) density-density correlations as a function of time and site offset.

velocity $v \approx 4Ja$, which is twice the maximum group velocity of a single particle with dispersion relation $\mathcal{E}_k = -2J \cos(ka)$. The correlations can spread with twice the velocity of a single particle since two lattice sites can be mutually influenced by signals from a source halfway between them. This is consistent with previous work describing the spread of correlations after a quench [83–87]. The transient correlations have a maximum amplitude which is controlled by U_0/T in the initial state, with correlations becoming suppressed as $U_0/T \rightarrow 0$. They reach this amplitude and then decay with a timescale proportional to $1/J$ in the postquench Hamiltonian.

In contrast to the low-temperature equilibrium state, the correlations are ferromagnetic rather than antiferromagnetic. Furthermore, the spin and density correlations are intertwined: the system develops positive spin-spin connected correlations and negative density-density connected correlations C_{ij}^{mm} of equal magnitude. The spin-spin correlations are independent of spin-orientation— $C_{ij}^{xx} = C_{ij}^{yy} = C_{ij}^{zz}$ and $C_{ij}^{a \neq b} = 0$ —since both the Hamiltonian and initial state are $SU(2)$ symmetric. The intertwined spin and density correlations stem from the fact that, in the noninteracting dynamics, there is only one energy scale, which is set by the postquench tunneling J . Thus, the spin and density correlations are controlled by the same energy scale.

To qualitatively understand the correlation dynamics, it is useful to consider the dynamics of a two-site model, which is shown schematically in Fig. 3. Let $|pq\rangle$ denote a state with

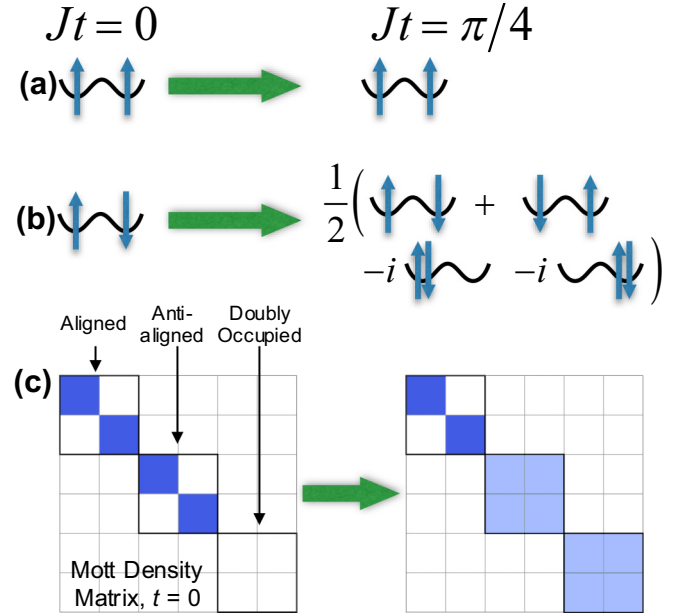


FIG. 3. Schematic diagram of the time evolution of a two-site model at unit filling, initially with $J_0 \ll T \ll U_0$, and then quenched to $U = 0$. (a) Aligned initial states do not evolve. (b) Anti-aligned initial states (the two-site equivalent of antiferromagnetic product states) evolve into superpositions with weight on doubly occupied states at later times. (c) The Mott-insulator-like initial density matrix on two sites transfers some weight from its matrix elements for anti-aligned states to doubly occupied states at later times, while aligned states’ matrix elements do not change. The matrix elements’ magnitudes are indicated by color, from white (zero) to dark blue (maximal).

p and q referring to the left and right sites, respectively, and taking on the values 0 (empty), \uparrow (one atom with spin up), \downarrow (one atom with spin down), and d (two atoms). The state $|\uparrow\uparrow\rangle$ does not evolve since Pauli blocking prevents it from coupling to any other states, while the state $|\uparrow\downarrow\rangle$ evolves in the Schrödinger picture as

$$|\uparrow\downarrow\rangle(Jt) = \cos^2(Jt)|\uparrow\downarrow\rangle_0 + \sin^2(Jt)|\downarrow\uparrow\rangle_0 - i \cos(Jt) \sin(Jt)(|d0\rangle_0 + |0d\rangle_0), \quad (19)$$

as shown in Figs. 3(a) and 3(b) for $Jt = \frac{\pi}{4}$. In Fig. 3(c), the ferromagnetic character of the dynamic spin correlations becomes apparent by observing that, although the initial density matrix has equal weight on aligned (e.g., $|\uparrow\uparrow\rangle$) and anti-aligned (e.g., $|\uparrow\downarrow\rangle$) spin configurations, the time-evolved matrix has more weight on the aligned states. This is because the aligned states stay frozen in time, while the anti-aligned states can partially convert to states with doublons and holes, reducing their spin correlations. The density correlations can be explained similarly: the initial density matrix has no weight on doubly occupied states, but the time-evolved matrix does. The double-occupancy next to a vacant site represents a negative two-site density correlation or, equivalently, a (short-ranged) density wave correlation.

Local observables approach constant values at large times. Although the noninteracting system is clearly integrable and thus not expected to thermalize, the expectation values of the

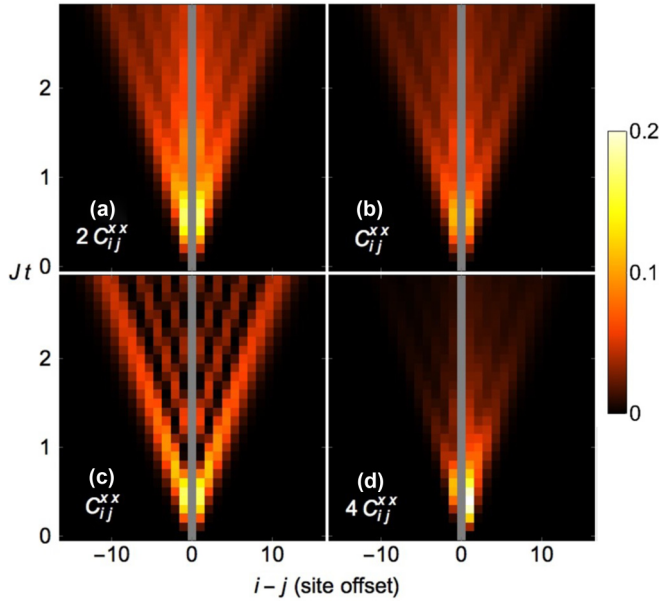


FIG. 4. Spreading of spin correlations is generic, demonstrated by four additional classes of initial conditions. (a) A $J_0 \ll T \ll U_0$ 1D hole-doped system, with $\langle n \rangle \approx 0.85$, (b) a $J_0 \ll T \ll U_0$ spin-imbalanced 1D system with $\langle \sigma^z \rangle \approx 0.25$, (c) a 1D product state antiferromagnet aligned along the z axis at half filling, and (d) a $J_0 \ll T \ll U_0$ 2D Mott insulator. In panel (d), site offsets to the right are along the $(1,0)$ direction, and those to the left are along $(1,1)$. In all cases, $\beta U_0 \rightarrow \infty$ in the initial state.

local observables as $t \rightarrow \infty$ are consistent with those of a thermal equilibrium state, in particular one at $T = \infty$. This occurs because the initial state is a product state in the site basis; thermalization is not expected for other, more general, initial states.

IV. QUENCHES FROM MORE GENERAL INITIAL STATES: DOPED AND SPIN-IMBALANCED SYSTEMS, TWO-DIMENSIONAL MOTT INSULATORS, AND ANTIFERROMAGNETS

The light-cone spreading of correlations from an uncorrelated initial state is not restricted to a one-dimensional (1D) Mott insulator, but also occurs for a variety of initial conditions, as shown in Fig. 4. We demonstrate this for a spin-imbalanced $T \gg J_0$ Mott insulator, a $T \gg J_0$ metal (with $n < 1$), a product state antiferromagnet, and a two-dimensional (2D) $T \gg J_0$ Mott insulator. We note that the metal can be alternatively viewed as a doped Mott insulator when $U_0 \gg J_0$.

Although both the spin-imbalanced and hole-doped 1D initial states show correlations developing in light cones as in the Mott insulator, the magnitude of the correlations is reduced, as shown in Fig. 4; this follows from Eq. (14) with the f and g in Eq. (15) evaluated in these limits (see below). One can induce a partially spin-polarized initial state by adding a term $B\sigma_i^z$ to Eq. (16) and likewise induce a number density other than one per site by taking the chemical potential to be $\mu = U_0/2 + \Delta$ with $\Delta \neq 0$.

For a partially spin-polarized system at unit filling, one finds

$$f_{\alpha\beta}^i = \frac{1}{\mathcal{N}_1} \delta_{\alpha\beta} (1 + e^{\frac{1}{2}\tilde{U}_0 + \frac{1}{2}\sigma_{\alpha\beta}^z \tilde{B}}), \quad (20a)$$

$$g_{\alpha\beta\gamma\delta}^j = \begin{cases} f_{\alpha\alpha}^i & \alpha = \beta = \gamma = \delta \\ \frac{1}{\mathcal{N}_1} & \alpha = \beta \neq \gamma = \delta \\ \frac{1}{\mathcal{N}_1} (1 + e^{\frac{1}{2}\tilde{U}_0 + \frac{1}{2}\sigma_{\alpha\delta}^z \tilde{B}}) & \alpha = \delta \neq \beta = \gamma \\ 0 & \text{otherwise,} \end{cases} \quad (20b)$$

with the normalization factor

$$\mathcal{N}_1 = 2 + 2 \exp\left(\frac{1}{2}\tilde{U}_0\right) \cosh\left(\frac{1}{2}\tilde{B}\right). \quad (21)$$

For a system doped away from unit filling,

$$f_{\alpha\beta}^i = \frac{1}{\mathcal{N}_2} \delta_{\alpha\beta} (e^{\tilde{\Delta}} + e^{\frac{1}{2}\tilde{U}_0}), \quad (22a)$$

$$g_{\alpha\beta\gamma\delta}^j = \begin{cases} f_{\alpha\alpha}^i & \alpha = \beta = \gamma = \delta \\ \frac{1}{\mathcal{N}_2} e^{\tilde{\Delta}} & \alpha = \beta \neq \gamma = \delta \\ \frac{1}{\mathcal{N}_2} e^{\frac{1}{2}\tilde{U}_0} & \alpha = \delta \neq \beta = \gamma \\ 0 & \text{otherwise,} \end{cases} \quad (22b)$$

with

$$\mathcal{N}_2 = 2 \left[\cosh(\tilde{\Delta}) + \exp\left(\frac{1}{2}\tilde{U}_0\right) \right]. \quad (23)$$

It is noteworthy that the phase and frequency of the oscillatory dynamics as well as the light cone velocity are independent of the doping and spin imbalance, which can be seen in Figs. 2 and 4. This is due to the fact that all the time dependence in Eq. (14) is contained in the single-particle propagators. Translationally invariant f and g can be factored out of each summation in Eq. (14) and their exact values do not qualitatively change the time evolution, except in fine-tuned limiting cases, e.g., a band insulator that has no time evolution. The values of f and g merely set the relative weight of each of the three time-dependent functions in Eq. (14). One important experimental consequence of this is that the transient dynamics described here is insensitive to spatial averaging across a trapped population of cold atoms (different locations in the trap will vary in number density and possibly in polarization).

Finally, for dynamics initiated from a 1D antiferromagnetic product state given by

$$\rho = \bigotimes_i \begin{cases} |\uparrow\rangle_i \langle \uparrow|_i & i \text{ even} \\ |\downarrow\rangle_i \langle \downarrow|_i & i \text{ odd,} \end{cases} \quad (24)$$

one finds

$$f_{\alpha\beta}^i = \begin{cases} \delta_{\alpha\beta} \delta_{\alpha\uparrow} & i \text{ even} \\ \delta_{\alpha\beta} \delta_{\alpha\downarrow} & i \text{ odd,} \end{cases} \quad (25a)$$

$$g_{\alpha\beta\gamma\delta}^j = f_{\alpha\delta}^i \delta_{\beta\gamma}. \quad (25b)$$

Unlike the other initial states described in this work, the antiferromagnetic product state is not a thermal state of a translationally invariant Hamiltonian. It can however be viewed as the thermal equilibrium state of the Hamiltonian H with the addition of a term $(-1)^j B \sigma_j^z$ in the limit that $B \rightarrow \infty$.

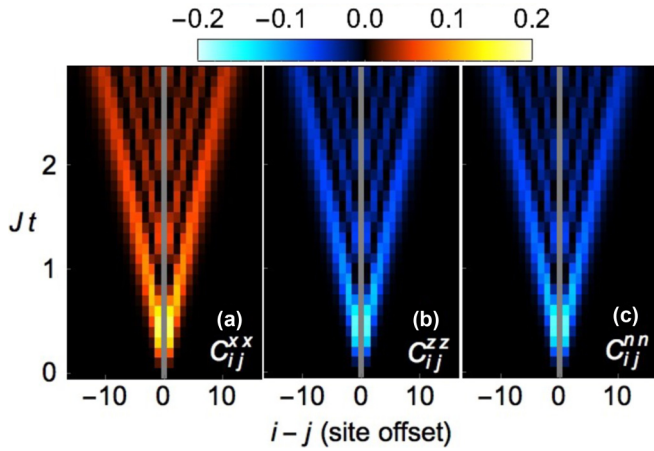


FIG. 5. Spreading of correlations in a 1D product state antiferromagnet aligned along the z axis. (a) Spin-spin correlations in the x direction C_{ij}^{xx} . The y - y correlations are identical: $C_{ij}^{yy} = C_{ij}^{xx}$ (b) Spin-spin correlations in the z direction C_{ij}^{zz} . (c) Density-density correlations C_{ij}^{nn} .

The antiferromagnet-initiated dynamics displays a distinctive feature: anisotropy in the spin correlations. As shown in Fig. 5, the C^{xx} and C^{yy} connected correlations remain positive and equal in magnitude, as they were in previous cases, but the C^{zz} and C^{nn} connected correlations are negative. They are, however, still equal in magnitude. The magnitudes of the correlations are larger than those of the 1D Mott insulator. The anisotropy manifests despite the $SU(2)$ symmetry of the Hamiltonian due to the broken symmetry of the initial state. Additionally, the correlations are strongest at the edge of the light cone, in contrast with the correlations of the translationally invariant 1D initial states which are strongest near the center of the light cone.

The light-cone spreading of correlations is not restricted to one-dimensional systems. As seen in Fig. 4(d), a two-dimensional Mott insulator on a square lattice shows qualitatively similar dynamics but develops weaker transient correlations than a 1D Mott insulator with the same postquench tunneling amplitude J .

In a two-dimensional Mott insulator, the initial expectation values do not differ from the 1D case, but the propagators take a different form. For a square lattice, they are

$$A_{pq}(t) = A_{p_x q_x}(t) A_{p_y q_y}(t), \quad (26)$$

where p and q are integer vectors indicating sites on the square lattice. Note that the 2D propagators factor into 1D components in this way due to the properties of the square lattice. It could be interesting to explore the effects of other geometries, where interference between different paths can give propagators with structures other than Eq. (26).

V. HOLE TRANSPORT DYNAMICS

Now we consider a system in which a single hole is added, localized to a single site, to the $T \gg J_0$ Mott insulator state discussed in Sec. III. The behavior of hole defects in fermionic

systems underpins the physics of many strongly correlated materials, where doping Mott insulators leads to a panoply of intriguing phenomena, most famously high-temperature superconductivity. The topic has long been of interest [88,89], and thermodynamics, spectral properties, and dynamics have been investigated [90–93]. It has recently been shown that a hole defect in a Mott insulating system disperses neither purely ballistically nor diffusively: the hole in fact leaves a trace in the background as it travels, preventing the quantum interference of some trajectories [94]. In light of this interesting result it is useful to consider the noninteracting analog.

The initial density matrix for a hole initially at site j_0 in a $T \gg J_0$ Mott insulator is

$$\rho = Z^{-1} \bigotimes_i \begin{cases} |0\rangle_i \langle 0|_i & i = j_0 \\ \exp(-\beta H_i) & \text{otherwise,} \end{cases} \quad (27)$$

which is identical to the Mott insulator density matrix except at j_0 . Likewise f^{j_0} and g^{j_0} are zero, with f and g otherwise identical to those of the Mott insulator.

We find that, as expected for single-particle ballistic motion, the hole disperses outwards according to the distribution

$$1 - \langle n_j \rangle(t) = |\mathcal{J}_{|j-j_0|}(2Jt)|^2, \quad (28)$$

as shown in Fig. 6(a).

Figure 6(b) shows that, as the hole disperses, it modifies spin correlations between pairs of nearby sites. In particular, the correlations obtain contributions of the opposite sign, suppressing the correlations and even at some points reversing their sign, compared with their values in the absence of the hole. This gives the impression that the spreading hole is dressed with a cloud of spin correlations. Such a phenomenon might be thought to be unique to an interacting system and is certainly of interest there. Our results show that apparently similar phenomena occur even without interactions, although they arise from different causes.

VI. CONCLUSIONS

We have shown that interaction quenches of the Fermi-Hubbard model from initial product states to the noninteracting limit produce transient connected two-site correlations. The correlations develop despite the initial states being at high temperature or, in the case of the product state antiferromagnet, high energy. Even when the temperature is much greater than the initial tunneling, and very much greater than the superexchange energy scale, significant correlations exist in the dynamics.

This finding contrasts with the natural idea that, at high temperature or high entropy, correlations should be absent. For example, in the context of previous work that has observed correlations out of equilibrium from a high-entropy initial state of ultracold molecules [95–97] it has sometimes been argued that long-range interactions are crucial. Our present work shows that, in contrast, correlations are ubiquitous out of equilibrium, even when one starts from high-entropy states.

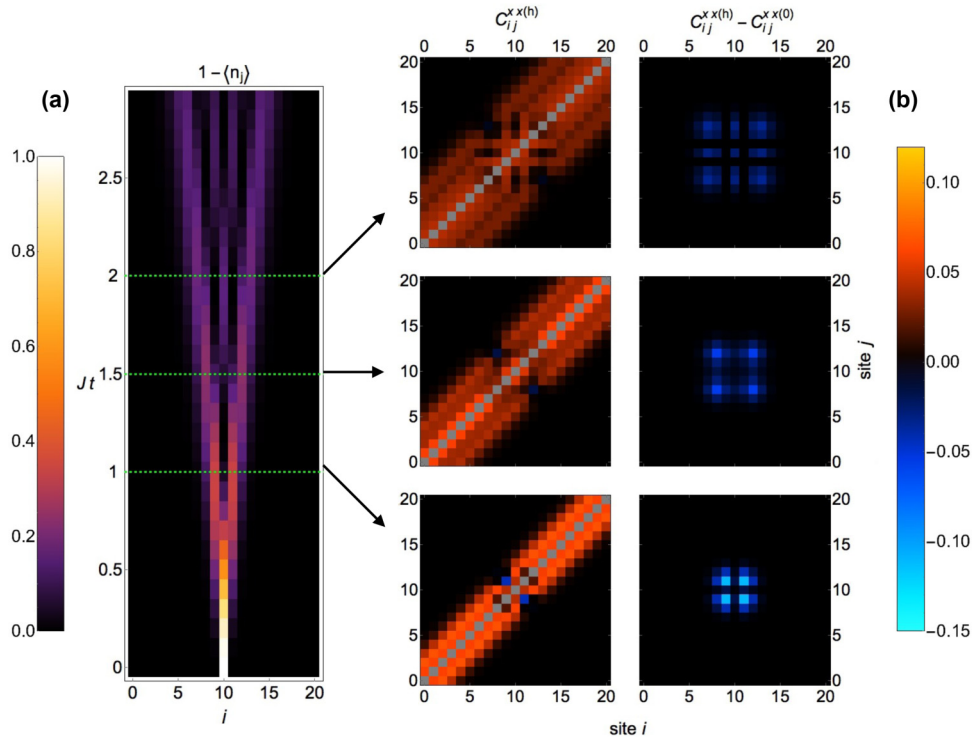


FIG. 6. Dynamics of a hole initially at $j_0 = 10$ on a $J_0 \ll T \ll U_0$ Mott insulating background after quenching to $U = 0$, and the hole's influence on spin correlations. (a) Hole density $1 - \langle n_j \rangle$. (b) Connected spin correlations C_{ij}^{xx} (left) and the difference in connected correlations between this system and a uniform system, with no hole (right). These are shown at the times $Jt = 1$ (bottom), $Jt = 1.5$ (middle), and $Jt = 2$ (top). The center of each plot in panel (b) corresponds to $i = j = 10$.

We generally observe that the correlations grow in a light cone and then fade away. In the process, interesting structures emerge, such as correlations with a sign opposite that of the equilibrium system and intertwined density and spin correlations of equal magnitude. It is noteworthy that these and other phenomena, such as the appearance of a spin correlation cloud around a hole, that look intriguing and might typically be associated with strong interactions, can occur quite generally in out-of-equilibrium systems, even in the absence of interactions. In this light, our work provides a useful comparison for future work with interacting quenches.

We note that the peak magnitudes of the connected correlations are up to about ~ 0.15 . While the precise values depend strongly on the initial conditions, these values are comparable in magnitude to recent equilibrium observations of correlations in 1D [52,55], 2D [57–59,62,74], and three dimensions (3D) [47,49,51,63,75,98,99]. This indicates that the correlations generated dynamically from uncorrelated initial states are large enough to be experimentally measured.

The analytic solution we describe here can be extended with some modification to certain initial states which are not single-site product states. Strictly nonoverlapping finite-range correlations, such as the correlation between adjacent sites that form a singlet, can be included in future studies by treating the correlated regions as sites in a superlattice.

Another interesting future direction involves understanding how the features of integrability of this system manifest for

finite-temperature initial states. This is much less explored than quenches from low-temperature initial states. It is expected to be fruitful to start by understanding the simplest integrable systems—noninteracting ones. For all the initial states we study, even though one expects the steady state to be nonthermal, i.e., to prethermalize, due to our initial conditions the prethermalization coincides with a $T = \infty$ thermal equilibrium state as measured by spin, density, and correlation operators. This is because the initial product state has equal overlap with all the states in the noninteracting band (i.e., the eigenstates of the final Hamiltonian), leading to a final state with occupation numbers independent of energy. We expect that perturbing the initial state away from a perfect product state will lead to a detectable difference from a thermal steady state. Likewise, including weak interactions in the postquench Hamiltonian should allow for the investigation of integrability breaking and prethermalization.

ACKNOWLEDGMENTS

We thank Rafael Polisele-Teles for conversations. K.R.A.H. thanks the Aspen Center for Physics, which is supported by National Science Foundation Grant No. PHY-1066293, for its hospitality while part of this work was carried out, and the Welch foundation, Grant No. C-1872. R.G.H. thanks the National Science Foundation (Grant No. PHY-1408309), the Welch Foundation (Grant No. C-1133), an ARO-MURI (Grant No. W911NF-14-1-0003), and the ONR.

- [1] T. Kinoshita, T. Wenger, and D. S. Weiss, *Nature (London)* **440**, 900 (2006).
- [2] M. Rigol, V. Dunjko, V. Yurovsky, and M. Olshanii, *Phys. Rev. Lett.* **98**, 050405 (2007).
- [3] U. Schneider, L. Hackermüller, J. P. Ronzheimer, S. Will, S. Braun, T. Best, I. Bloch, E. Demler, S. Mandt, D. Rasch, and A. Rosch, *Nat. Phys.* **8**, 213 (2012).
- [4] J. Marino and A. Silva, *Phys. Rev. B* **89**, 024303 (2014).
- [5] A. Bauer, F. Dorfner, and F. Heidrich-Meisner, *Phys. Rev. A* **91**, 053628 (2015).
- [6] L. Riegger, G. Orso, and F. Heidrich-Meisner, *Phys. Rev. A* **91**, 043623 (2015).
- [7] M. Moeckel and S. Kehrein, *Phys. Rev. Lett.* **100**, 175702 (2008).
- [8] J. M. Zhang, C. Shen, and W. M. Liu, *Phys. Rev. A* **83**, 063622 (2011).
- [9] M. Babadi, E. Demler, and M. Knap, *Phys. Rev. X* **5**, 041005 (2015).
- [10] M. Schulz, C. A. Hooley, and R. Moessner, *Phys. Rev. A* **94**, 063643 (2016).
- [11] J. Eisert, M. Friesdorf, and C. Gogolin, *Nat. Phys.* **11**, 124 (2015).
- [12] N. Fläschner, D. Vogel, M. Tarnowski, B. S. Rem, D. S. Lühmann, M. Heyl, J. C. Budich, L. Mathey, K. Sengstock, and C. Weitenberg, *Nat. Phys.* **14**, 265 (2018).
- [13] K. Mikelson, J. K. Freericks, and H. R. Krishnamurthy, *Phys. Rev. Lett.* **109**, 260402 (2012).
- [14] L. Mathey and A. Polkovnikov, *Phys. Rev. A* **80**, 041601(R) (2009).
- [15] U. Ebling, J. S. Krauser, N. Fläschner, K. Sengstock, C. Becker, M. Lewenstein, and A. Eckardt, *Phys. Rev. X* **4**, 021011 (2014).
- [16] P. W. Anderson, *Phys. Rev.* **109**, 1492 (1958).
- [17] D. Basko, I. Aleiner, and B. Altshuler, *Ann. Phys. (NY)* **321**, 1126 (2006).
- [18] A. C. Cassidy, C. W. Clark, and M. Rigol, *Phys. Rev. Lett.* **106**, 140405 (2011).
- [19] R. Nandkishore and D. A. Huse, *Annu. Rev. Condens. Matter Phys.* **6**, 15 (2015).
- [20] A. Pal and D. A. Huse, *Phys. Rev. B* **82**, 174411 (2010).
- [21] A. Polkovnikov, K. Sengupta, A. Silva, and M. Vengalattore, *Rev. Mod. Phys.* **83**, 863 (2011).
- [22] F. H. L. Essler, S. Kehrein, S. R. Manmana, and N. J. Robinson, *Phys. Rev. B* **89**, 165104 (2014).
- [23] M. Cramer, C. M. Dawson, J. Eisert, and T. J. Osborne, *Phys. Rev. Lett.* **100**, 030602 (2008).
- [24] F. Queisser, K. V. Krutitsky, P. Navez, and R. Schützhold, *Phys. Rev. A* **89**, 033616 (2014).
- [25] M. Eckstein, M. Kollar, and P. Werner, *Phys. Rev. Lett.* **103**, 056403 (2009).
- [26] J.-y. Choi, S. Hild, J. Zeiher, P. Schauß, A. Rubio-Abadal, T. Yefsah, V. Khemani, D. A. Huse, I. Bloch, and C. Gross, *Science* **352**, 1547 (2016).
- [27] D. M. Kennes, J. C. Pommerening, J. Diekmann, C. Karrasch, and V. Meden, *Phys. Rev. B* **95**, 035147 (2017).
- [28] X. Yin and L. Radzihovsky, *Phys. Rev. A* **94**, 063637 (2016).
- [29] M. Kollar and M. Eckstein, *Phys. Rev. A* **78**, 013626 (2008).
- [30] I. V. Gornyi, A. D. Mirlin, and D. G. Polyakov, *Phys. Rev. Lett.* **95**, 206603 (2005).
- [31] M. Serbyn, Z. Papić, and D. A. Abanin, *Phys. Rev. Lett.* **111**, 127201 (2013).
- [32] D. A. Huse, R. Nandkishore, V. Oganesyan, A. Pal, and S. L. Sondhi, *Phys. Rev. B* **88**, 014206 (2013).
- [33] D. A. Huse, R. Nandkishore, and V. Oganesyan, *Phys. Rev. B* **90**, 174202 (2014).
- [34] J. H. Bardarson, F. Pollmann, and J. E. Moore, *Phys. Rev. Lett.* **109**, 017202 (2012).
- [35] R. Vosk and E. Altman, *Phys. Rev. Lett.* **110**, 067204 (2013).
- [36] M. Serbyn, Z. Papić, and D. A. Abanin, *Phys. Rev. Lett.* **110**, 260601 (2013).
- [37] A. Nanduri, H. Kim, and D. A. Huse, *Phys. Rev. B* **90**, 064201 (2014).
- [38] M. Schreiber, S. S. Hodgman, P. Bordia, H. P. Lüschen, M. H. Fischer, R. Vosk, E. Altman, U. Schneider, and I. Bloch, *Science* **349**, 842 (2015).
- [39] S. S. Kondov, W. R. McGehee, W. Xu, and B. DeMarco, *Phys. Rev. Lett.* **114**, 083002 (2015).
- [40] M. Mitrano, A. Cantaluppi, D. Nicoletti, S. Kaiser, A. Perucchi, S. Lupi, P. Di Pietro, D. Pontiroli, M. Riccò, S. R. Clark, D. Jaksch, and A. Cavalleri, *Nature (London)* **530**, 461 (2016).
- [41] D. N. Basov, R. D. Averitt, D. van der Marel, M. Dressel, and K. Haule, *Rev. Mod. Phys.* **83**, 471 (2011).
- [42] D. Nicoletti and A. Cavalleri, *Adv. Opt. Photonics* **8**, 401 (2016).
- [43] C. Giannetti, M. Capone, D. Fausti, M. Fabrizio, F. Parmigiani, and D. Mihailovic, *Adv. Phys.* **65**, 58 (2016).
- [44] M. Schiró and M. Fabrizio, *Phys. Rev. Lett.* **105**, 076401 (2010).
- [45] J. Bauer, M. Babadi, and E. Demler, *Phys. Rev. B* **92**, 024305 (2015).
- [46] P. M. Duarte, R. A. Hart, T.-L. Yang, X. Liu, T. Paiva, E. Khatami, R. T. Scalettar, N. Trivedi, and R. G. Hulet, *Phys. Rev. Lett.* **114**, 070403 (2015).
- [47] R. A. Hart, P. M. Duarte, T.-L. Yang, X. Liu, T. Paiva, E. Khatami, R. T. Scalettar, N. Trivedi, D. A. Huse, and R. G. Hulet, *Nature (London)* **519**, 211 (2015).
- [48] R. Jordens, N. Strohmaier, K. Gunter, H. Moritz, and T. Esslinger, *Nature (London)* **455**, 204 (2008).
- [49] D. Greif, T. Uehlinger, G. Jotzu, L. Tarruell, and T. Esslinger, *Science* **340**, 1307 (2013).
- [50] R. Jordens, L. Tarruell, D. Greif, T. Uehlinger, N. Strohmaier, H. Moritz, T. Esslinger, L. De Leo, C. Kollath, A. Georges, V. Scarola, L. Pollet, E. Burovski, E. Kozik, and M. Troyer, *Phys. Rev. Lett.* **104**, 180401 (2010).
- [51] J. Imriška, M. Iazzi, L. Wang, E. Gull, D. Greif, T. Uehlinger, G. Jotzu, L. Tarruell, T. Esslinger, and M. Troyer, *Phys. Rev. Lett.* **112**, 115301 (2014).
- [52] D. Greif, G. Jotzu, M. Messer, R. Desbuquois, and T. Esslinger, *Phys. Rev. Lett.* **115**, 260401 (2015).
- [53] U. Schneider, L. Hackermüller, S. Will, T. Best, I. Bloch, T. A. Costi, R. W. Helmes, D. Rasch, and A. Rosch, *Science* **322**, 1520 (2008).
- [54] L. Hackermüller, U. Schneider, M. Moreno-Cardoner, T. Kitagawa, T. Best, S. Will, E. Demler, E. Altman, I. Bloch, and B. Paredes, *Science* **327**, 1621 (2010).
- [55] M. Boll, T. A. Hilker, G. Salomon, A. Omran, J. Nespolo, L. Pollet, I. Bloch, and C. Gross, *Science* **353**, 1257 (2016).
- [56] L. W. Cheuk, M. A. Nichols, M. Okan, T. Gersdorf, V. V. Ramasesh, W. S. Bakr, T. Lompe, and M. W. Zwierlein, *Phys. Rev. Lett.* **114**, 193001 (2015).

- [57] L. W. Cheuk, M. A. Nichols, K. R. Lawrence, M. Okan, H. Zhang, E. Khatami, N. Trivedi, T. Paiva, M. Rigol, and M. W. Zwierlein, *Science* **353**, 1260 (2016).
- [58] D. Greif, M. F. Parsons, A. Mazurenko, C. S. Chiu, S. Blatt, F. Huber, G. Ji, and M. Greiner, *Science* **351**, 953 (2016).
- [59] M. F. Parsons, A. Mazurenko, C. S. Chiu, G. Ji, D. Greif, and M. Greiner, *Science* **353**, 1253 (2016).
- [60] S. Taie, R. Yamazaki, S. Sugawa, and Y. Takahashi, *Nat. Phys.* **8**, 825 (2012).
- [61] C. Hofrichter, L. Riegger, F. Scazza, M. Höfer, D. R. Fernandes, I. Bloch, and S. Fölling, *Phys. Rev. X* **6**, 021030 (2016).
- [62] E. Cocchi, L. A. Miller, J. H. Drewes, M. Koschorreck, D. Pertot, F. Brennecke, and M. Köhl, *Phys. Rev. Lett.* **116**, 175301 (2016).
- [63] J. H. Drewes, E. Cocchi, L. A. Miller, C. F. Chan, D. Pertot, F. Brennecke, and M. Köhl, *Phys. Rev. Lett.* **117**, 135301 (2016).
- [64] J. H. Drewes, L. A. Miller, E. Cocchi, C. F. Chan, N. Wurz, M. Gall, D. Pertot, F. Brennecke, and M. Köhl, *Phys. Rev. Lett.* **118**, 170401 (2017).
- [65] T. Esslinger, *Annu. Rev. Condens. Matter Phys.* **1**, 129 (2010).
- [66] M. Ojekhile, R. Höppner, H. Moritz, and L. Mathey, *Z. Naturforsch. A* **71**, 1143 (2016).
- [67] T.-L. Ho, [arXiv:0808.2677](https://arxiv.org/abs/0808.2677).
- [68] M. Lubasch, V. Murg, U. Schneider, J. I. Cirac, and M.-C. Bañuls, *Phys. Rev. Lett.* **107**, 165301 (2011).
- [69] E. Fradkin, S. A. Kivelson, and J. M. Tranquada, *Rev. Mod. Phys.* **87**, 457 (2015).
- [70] D. Jaksch, C. Bruder, J. I. Cirac, C. W. Gardiner, and P. Zoller, *Phys. Rev. Lett.* **81**, 3108 (1998).
- [71] G. Modugno, F. Ferlaino, R. Heidemann, G. Roati, and M. Inguscio, *Phys. Rev. A* **68**, 011601(R) (2003).
- [72] M. Köhl, H. Moritz, T. Stöferle, K. Günter, and T. Esslinger, *Phys. Rev. Lett.* **94**, 080403 (2005).
- [73] M. Endres, M. Cheneau, T. Fukuhara, C. Weitenberg, P. Schauß, C. Gross, L. Mazza, M. C. Bañuls, L. Pollet, I. Bloch, and S. Kuhr, *Appl. Phys. B: Lasers Opt.* **113**, 27 (2013).
- [74] P. T. Brown, D. Mitra, E. Guardado-Sanchez, P. Schauß, S. S. Kondov, E. Khatami, T. Paiva, N. Trivedi, D. A. Huse, and W. S. Bakr, *Science* **357**, 1385 (2017).
- [75] D. Greif, L. Tarruell, T. Uehlinger, R. Jördens, and T. Esslinger, *Phys. Rev. Lett.* **106**, 145302 (2011).
- [76] H.-N. Dai, B. Yang, A. Reingruber, X.-F. Xu, X. Jiang, Y.-A. Chen, Z.-S. Yuan, and J.-W. Pan, *Nat. Phys.* **12**, 783 (2016).
- [77] E. Altman, E. Demler, and M. D. Lukin, *Phys. Rev. A* **70**, 013603 (2004).
- [78] L. Mathey, A. Vishwanath, and E. Altman, *Phys. Rev. A* **79**, 013609 (2009).
- [79] M. Gluza, C. Krumnow, M. Friesdorf, C. Gogolin, and J. Eisert, *Phys. Rev. Lett.* **117**, 190602 (2016).
- [80] P. Makotyn, C. E. Klauss, D. L. Goldberger, E. A. Cornell, and D. S. Jin, *Nat. Phys.* **10**, 116 (2014).
- [81] L. W. Cheuk, M. A. Nichols, K. R. Lawrence, M. Okan, H. Zhang, and M. W. Zwierlein, *Phys. Rev. Lett.* **116**, 235301 (2016).
- [82] F. Werner, O. Parcollet, A. Georges, and S. R. Hassan, *Phys. Rev. Lett.* **95**, 056401 (2005).
- [83] P. Calabrese and J. Cardy, *Phys. Rev. Lett.* **96**, 136801 (2006).
- [84] M. Cheneau, P. Barmettler, D. Poletti, M. Endres, P. Schausz, T. Fukuhara, C. Gross, I. Bloch, C. Kollath, and S. Kuhr, *Nature (London)* **481**, 484 (2012).
- [85] S. Porta, F. M. Gambetta, F. Cavaliere, N. Traverso Ziani, and M. Sasseti, *Phys. Rev. B* **94**, 085122 (2016).
- [86] R. Geiger, T. Langen, I. E. Mazets, and J. Schmiedmayer, *New J. Phys.* **16**, 053034 (2014).
- [87] T. Enss and J. Sirker, *New J. Phys.* **14**, 023008 (2012).
- [88] G. Montambaux, M. Héritier, and P. Lederer, *J. Low Temp. Phys.* **47**, 39 (1982).
- [89] S. A. Trugman, *Phys. Rev. B* **41**, 892 (1990).
- [90] N. V. Prokof'ev and P. C. E. Stamp, *Phys. Rev. A* **74**, 020102(R) (2006).
- [91] F. Trouselet, P. Horsch, A. M. Oleś, and W.-L. You, *Phys. Rev. B* **90**, 024404 (2014).
- [92] I. Kimchi, J. G. Analytis, and A. Vishwanath, *Phys. Rev. B* **90**, 205126 (2014).
- [93] G. B. Halász, J. T. Chalker, and R. Moessner, *Phys. Rev. B* **90**, 035145 (2014).
- [94] J. Carlström, N. Prokof'ev, and B. Svistunov, *Phys. Rev. Lett.* **116**, 247202 (2016).
- [95] B. Yan, S. A. Moses, B. Gadway, J. P. Covey, K. R. A. Hazzard, A. M. Rey, D. S. Jin, and J. Ye, *Nature (London)* **501**, 521 (2013).
- [96] A. de Paz, A. Sharma, A. Chotia, E. Maréchal, J. H. Huckans, P. Pedri, L. Santos, O. Gorceix, L. Vernac, and B. Laburthe-Tolra, *Phys. Rev. Lett.* **111**, 185305 (2013).
- [97] K. R. A. Hazzard, B. Gadway, M. Foss-Feig, B. Yan, S. A. Moses, J. P. Covey, N. Y. Yao, M. D. Lukin, J. Ye, D. S. Jin, and A. M. Rey, *Phys. Rev. Lett.* **113**, 195302 (2014).
- [98] S. Fuchs, E. Gull, L. Pollet, E. Burovski, E. Kozik, T. Pruschke, and M. Troyer, *Phys. Rev. Lett.* **106**, 030401 (2011).
- [99] T. Paiva, Y. L. Loh, M. Randeria, R. T. Scalettar, and N. Trivedi, *Phys. Rev. Lett.* **107**, 086401 (2011).